

## Two-dimensional resonant modes in stacked Josephson junctions

R. Kleiner\*

Walther-Meissner-Institut, D-85748 Garching, Germany

(Received 16 May 1994)

In a vertical stack of Josephson junctions, vortices in adjacent junctions are coupled by screening currents if the electrodes are thinner than the London penetration depth. We investigate typical junction parameters of both niobium multilayers and intrinsic Josephson junctions in high- $T_c$  single crystals. Using coupled one-dimensional sine-Gordon equations, stable coherent motion of Josephson vortices in an external magnetic field is predicted. This motion is triggered by two-dimensional resonances of the stack. For the resonance frequencies and amplitudes analytical expressions are derived.

Stacked Josephson junctions are valuable objects both for theoretical and experimental investigations at least for three reasons. First, nonlinear effects resulting from the sinusoidal current-phase relation of the Josephson currents and the dynamics of fluxoid quanta, moving along the barriers between the superconducting layers (Josephson vortices), can be studied in general. If the thicknesses of the superconducting layers  $d$  are much smaller than the magnetic penetration depth  $\lambda$ , screening currents flowing around Josephson vortex will spread over several junctions. Thus vortices moving along different junctions interact, one of the possible results being coherent motion of these vortices. Under appropriate conditions, Josephson vortices will excite cavity resonances of the stack (the Fiske resonances), which in turn influence the vortex motion. The existence as well as the stability of a coherent vortex motion has been shown for a stack of two junctions.<sup>1-3</sup> There are two different resonant modes in these stacks, a symmetric mode with equal electric fields across each junction and an asymmetric mode involving opposite equal fields.<sup>2,4</sup> *A priori*, it is unclear if similar results can be obtained for stacks of more than two junctions. The two-junction stack is symmetric in the sense that each junction has one outermost electrode and one electrode shared with the second junction. This symmetry is obviously broken in larger stacks.

The second reason is that many high- $T_c$  superconductors, e.g.,  $\text{Bi}_2\text{Sr}_2\text{CaCu}_2\text{O}_8$  (BSCCO), as well as some organic superconductors like  $\kappa$ -(BEDT-TTF)<sub>2</sub>Cu(NCS)<sub>2</sub>, act intrinsically as natural stacks of thousands of junctions.<sup>5</sup> In these materials, the ratio of the thickness of the superconducting layers (CuO<sub>2</sub> or BEDT-TTF layers respectively), and the field penetration depth  $\lambda$  is of the order of  $10^{-3}$  resulting in a strong coupling between different junctions. An analysis of stacked Josephson junctions will thus give insight into the electrodynamics of these important superconductors.

Third, there are promising applications of stacked Josephson junctions. Tunable high-frequency sources based on planar arrays of phase locked junctions already produce power levels of several  $\mu\text{W}$  into high-impedance loads (20–60  $\Omega$ ) in the submillimeter wave range.<sup>6</sup> Long Josephson junctions are used as fluxon oscillators, the os-

cillator frequency being controlled by an external magnetic field directed parallel to the layers.<sup>7</sup> Vertical packaging in arrays will help to increase the number of junctions, while keeping the array dimensions small. Stacking in the case of flux-flow oscillators helps increase their output power and decrease their impedance mismatch.

The purpose of this work is to show, both numerically and analytically, that under appropriate conditions the interaction due to screening currents should give rise to coherent motion of vortices in different junctions. We will show that coherent motion is promoted by two-dimensional resonances. These resonances are the two-dimensional analog of Fiske resonances known from single junctions.

We first introduce the model of coupled sine-Gordon equations describing the dynamics of stacked Josephson junctions,<sup>8,9</sup> which is derived for arbitrary ratios of the thickness of the superconducting electrodes and the London penetration depth  $\lambda$ . A schematic drawing of a stack of  $N$  Josephson junctions is shown in Fig. 1. For the sake of simplicity we write down the following equations for identical junction parameters. The time variable  $\tau$  is normalized to  $\Phi_0\sigma/(2\pi j_c t)$ ;  $\sigma$  is the electrical conductivity,  $j_c$  is the maximum density of the Josephson currents. Lengths are given in units of the junction length  $b$  in  $x$  direction, electrical fields  $e_{z,n}$  in units  $j_c/\sigma$ , magnetic fields  $h$  in units  $\Phi_0/(\mu_0 tb)$ , and current densities in units  $j_c$ . Integrating the phase gradient of the order parameter in the  $n$ th electrode,

$$\varphi'_n = 2\pi/\Phi_0 (A_{x,n} + \mu_0\lambda^2 j_{x,n}),$$

along the contour shown in Fig. 1, and using Maxwell's equations, yields the coupled sine-Gordon equations describing the dynamics of stacked Josephson junctions,

$$\gamma'' = M(\beta_c \dot{\gamma} + \dot{\gamma} + j^s - j_{\text{ext}}), \quad (1)$$

with the gauge-invariant phase differences  $\gamma = (\gamma_1, \dots, \gamma_N)$ ;  $j^s = (\sin\gamma_1, \dots, \sin\gamma_N)$ ,  $j_{\text{ext}} = j_{\text{ext}}(1, \dots, 1)$ .  $\beta_c = 2\pi\epsilon\epsilon_0 j_c t / \sigma^2 \Phi_0$  is the McCumber parameter;  $\epsilon$  is the dielectric constant. The elements of the matrix  $M$  are given by  $M_{ii} = (b/\lambda_j)^2$ ,  $M_{ii+1} = M_{ii-1} = -(b/\lambda_k)^2$ , with  $\lambda_j^{-2} = \lambda_m^{-2} + 2\lambda_k^{-2}$ ,

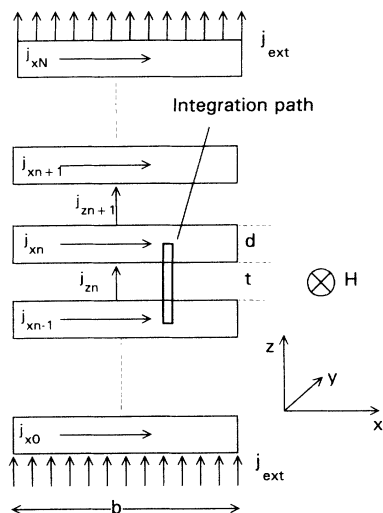


FIG. 1. Stack of  $N$  Josephson junctions in a magnetic field. The electrodes are numbered from 0 to  $N$ . The width of the stack in the  $x$  direction is  $b$ . Its width in the  $y$  direction,  $a$ , is assumed to be smaller than the characteristic correlation lengths  $\lambda_m$  and  $\lambda_k$  introduced in the text. Screening currents flowing along the  $n$ th electrode are denoted  $j_{x,n}$ . The  $z$ -axis currents  $j_{z,n}$  flowing across the  $n$ th Josephson junctions of the stack are given by the sum of Josephson currents, quasiparticle currents, and displacement currents. Transport currents with homogeneous density  $j_{\text{ext}}$  are fed into the outermost electrodes Nos. 0 and  $N$ . The external magnetic field is directed along the  $y$  parallel to the layers. The integration path (thick line) is used to obtain Eq. (1).

$\lambda_m = [\Phi_0 / (2\pi\mu_0 t_{\text{eff}} j_c)]^{1/2}$ ,  $\lambda_k = [(\Phi_0 d_{\text{eff}}) / (2\pi\mu_0 \lambda^2 j_c)]^{1/2}$ ,  $t_{\text{eff}} = t + 2\lambda \tanh[d / (2\lambda)]$ , and  $d_{\text{eff}} = \lambda \sinh(d / \lambda)$ . Other elements of  $M$  are zero. Boundary conditions are

$$\gamma'(x=0) = \gamma'(x=1) = 2\pi h_{\text{ext}} \mathbf{1}, \quad \mathbf{1} = (1, \dots, 1).$$

Equation (1) is the analog of the sine-Gordon equation of a single long Josephson junction of the overlap geometry.<sup>7</sup> The length  $\lambda_m$  describes the screening length for magnetic fields directed along  $y$ .<sup>9</sup>  $\lambda_j$  corresponds to the “core” diameter of the Josephson vortex in the static case.<sup>8</sup>

For Nb-Al/AIO<sub>x</sub>-Nb multilayers,<sup>2</sup> typical junction parameters are  $d = \lambda = 90$  nm,  $t = 2$  nm, and  $j_c = 250$  A/cm<sup>2</sup>. This yields  $\lambda_m = 33$   $\mu\text{m}$ ,  $\lambda_k = 37$   $\mu\text{m}$ , and  $\lambda_j = 21$   $\mu\text{m}$ . For intrinsic Josephson junctions in BSCCO we have  $d = 3$   $\text{\AA}$ ,  $t = 12$   $\text{\AA}$ ,  $\lambda = 1700$   $\text{\AA}$ , and  $j_c = 150$  A/cm<sup>2</sup>. For these stacks we thus get  $\lambda_m = 340$   $\mu\text{m}$ ,  $\lambda_k = 1.5$   $\mu\text{m}$ , and  $\lambda_j = 1.1$   $\mu\text{m}$ .

The coupled sine-Gordon equations have been solved numerically for stacks of up to  $N = 19$  junctions. For the numerical treatment Eq. (1) has been decomposed into Fourier components as described in Ref. 9. For the simulations shown below we used 40 Fourier components. The McCumber parameter is  $\beta_c = 100$ , i.e., we investigate the underdamped case, where ballistic vortex dynamics takes place. The simulations were performed both with parameters typical for the weakly coupled (i.e.,  $d \approx \lambda$ ) Nb

multilayers ( $\lambda_m = 33$   $\mu\text{m}$ ,  $\lambda_k = 37$   $\mu\text{m}$ ,  $\lambda_j = 21$   $\mu\text{m}$ ,  $b = 100$   $\mu\text{m}$ ) and with parameters typical for the strongly coupled ( $d \ll \lambda$ ) intrinsic Josephson junctions in BSCCO ( $\lambda_m = 340$   $\mu\text{m}$ ,  $\lambda_k = 1.5$   $\mu\text{m}$ ,  $\lambda_j = 1.1$   $\mu\text{m}$ ,  $b = 20$   $\mu\text{m}$ ). For all simulations a parameter spread of 5% has been used.

We emphasize, that for Nb parameters both the width of the stack  $b$  and its thickness are large compared to  $\lambda_m$  and  $\lambda$ , respectively. In contrast, for BSCCO parameters, the stack is much thinner than  $\lambda$ , and its width,  $b$ , is much smaller than  $\lambda_m$  but larger than  $\lambda_j$ . In this situation only a tiny fraction of an external field is screened, although screening currents still vary on the short scale of  $\lambda_j$ . This situation is different from fluxon dynamics in standard long Josephson junctions. Nevertheless, we want to refer to vortices arising from this situation as “Josephson vortices.”

The results can be summarized as follows.

(1) In zero or weak magnetic fields there are only few stable phase-locked modes with vortices located in different junctions. An example is the motion of three vortex-antivortex pairs in a stack of five junctions.<sup>9</sup> Coherent modes, e.g., one vortex moving in each junction, turned out to be stable only in the  $N = 2$  case.<sup>8,9</sup>

(2) Stable collective modes exist in the flux-flow regime for  $h_{\text{ext}} \gg 1$ . Josephson vortices can excite cavity resonances of the whole stack, which in turn trigger the motion of vortices. At the resonances the electrical field is approximately given by

$$E_{z,n} \approx E_z^0 + E_{z,n}^1 \cos(\pi k_x x) \cos(\omega t),$$

with  $k_x = 1, 2, \dots$ . We note that  $k_x$  does not depend on the junction number  $n$ . The amplitudes  $E_{z,n}^1$  vary approximately sinusoidally,  $E_{z,n}^1 \approx \tilde{E}_z \sin[\pi k_z n / (N + 1)]$ , with  $k_z = 1, 2, \dots$ .

These collective resonances have found to be stable both in weakly coupled and strongly coupled stacks. As an example, Fig. 2 shows a mode with  $k_x = 9$  and  $k_z = 3$ . The simulation has been done for a stack of 19 strongly coupled junctions. The external magnetic field is  $h_{\text{ext}} = 5$ ; the bias current is  $j_{\text{ext}} = 0.6$ . The left part of the figure shows the Josephson currents  $j_{z,n}^s$  of all junctions; the right part shows the electrical fields. Black dots mark the center of mass of the Josephson vortices, where  $\gamma_n = (2l + 1)\pi$ ,  $l = 0, 1, 2, \dots$ . The vortices are aligned in three domains (junction Nos. 2–5, 8–11, and 15–18). Vortices of the second group move with a phase shift of  $\pi$  with respect to the other groups. Vortices moving in junctions where the amplitude of the electrical field is small (i.e., junction Nos. 1, 6, 7, 12–14, and 19) are not locked to the standing wave pattern. For the  $N = 2$  case such a bunched movement of fluxons has been shown analytically to be stable.<sup>1</sup> Figure 3 shows the superposition of the corresponding  $I-V$  characteristics of all junctions for  $h_{\text{ext}} = 5$ . Resonances show up as current steps. Note that the average voltage drop across unlocked junctions is larger than the voltage drop across locked junctions. Besides the resonance shown in Fig. 3, resonances with  $k_x$  between 8 and 10 and  $k_z$  of 2 and 3 have also found to be stable for this special value of the external

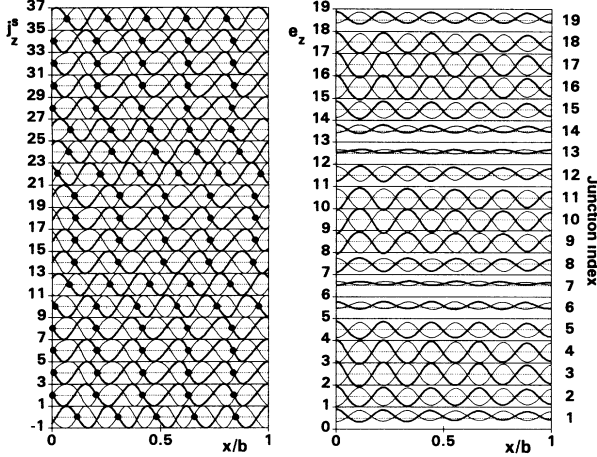


FIG. 2. Simulation of a stack of  $N=19$  strongly coupled Josephson junctions with the parameters given in the text. The left part of the figure shows the Josephson currents  $j_{z,n}^j$  vs the  $x$  coordinate of the stack. All curves have been vertically offset proportional to the junction index in order to map the junctions of the stack. Thick and thin curves correspond to two different values of the normalized time  $\tau=26$  and  $32$ . In order to show that the Josephson vortices move in three aligned domains the centers of mass of the vortices have been marked with black dots for  $\tau=26$ . The right part of the figure shows the electrical field component in  $z$  direction  $e_{z,n}$ . The figure shows that a two-dimensional standing wave pattern has developed. In the  $n$ th junction the electrical field is approximately of the form  $e_n \approx e_0 + \bar{e}_1 \sin[\pi k_z / (N+1)] \cos(\pi k_x x) \cos(e_0 \tau)$  with  $k_x=9$  and  $k_z=3$ .

magnetic field. Varying the external field, a large number of different resonances can be stabilized including the  $k_z=1$  mode, where almost all vortices, except the ones moving in the outermost junctions, move in phase.

In order to find analytical expressions for the resonance frequencies we approximate the electrical field by

$$\dot{\gamma}(x, \tau) = e_0 1 + e_1 \cos(\pi k_x x) \cos(e_0 \tau), \quad k_x = 0, 1, 2, \dots,$$

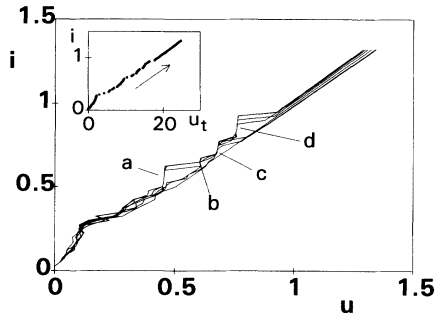


FIG. 3. Normalized bias current  $i = I/I_c$  vs normalized voltage  $u = U/U_c$  of all of the junctions of the  $N=19$  stack. The external field is  $h_{\text{ext}}=5$ . The inset shows  $i$  vs the total voltage across the stack  $u_t$ . Junction parameters are the same as in Fig. 2. Different cavity resonances showing up as current steps are denoted  $a-d$ . The  $k_x$  and  $k_z$  values are (a)  $k_x=9$ ,  $k_z=3$ , (b)  $k_x=8$ ,  $k_z=2$ , (c)  $k_x=9$ ,  $k_z=2$ , and (d)  $k_x=10$ ,  $k_z=2$ .

which yields

$$\gamma(x, \tau) = e_0 \tau + \frac{e_1}{e_0} \cos(\pi k_x x) \sin(e_0 \tau) + 2\pi h_{\text{ext}} x + g_0. \quad (2)$$

The following approach is very similar to Kulik's approach for the single-junction case.<sup>10</sup> It is strictly valid only if magnetic fields of currents flowing along  $z$  are small. This condition is normally fulfilled at least for the strongly coupled intrinsic Josephson junctions, where typical crystal dimensions are much smaller than  $\lambda_m$ . Inserting Eq. (2) in Eq. (1), multiplying with  $\cos(\pi k_x x)$  and integrating along  $x$  from 0 to 1 yields

$$e_1 \frac{\pi^2 k_x^2}{e_0} \sin(e_0 \tau) = M [\beta_c e_0 e_1 \sin(e_0 \tau) - e_1 \cos(e_0 \tau) - 2I], \quad (3)$$

$$I_n = \text{Im} \left[ e^{ie_0 \tau} e^{ig_n} \times \int_0^1 dx [e^{i\Theta_n \cos \pi k_x x} e^{i2\pi h_{\text{ext}} x} \cos(\pi k_x x)] \right],$$

$$\Theta_n = \frac{e_{1,n}}{e_0} \sin(e_0 \tau).$$

We neglect the contribution to  $I=(I_1, \dots, I_N)$  oscillating proportional to  $\sin(e_0 \tau)$  for  $\beta_c \gg 1$ . From Eq. (3) we then get the eigenvalue equation:

$$M e_1 = \frac{\pi^2 k_x^2}{\beta_c e_0^2} e_1 \quad (4)$$

with the solution

$$e_{1,n} = \bar{e}_1 \sin \left[ \frac{n \pi k_z}{N+1} \right] \quad (5a)$$

$$e_0 = \frac{\lambda_k \pi k_x}{b \sqrt{\beta_c}} \frac{1}{\sqrt{(\lambda_k / \lambda_m)^2 + 2[1 - \cos(\pi k_z / (N+1))]}}, \quad (5b)$$

$n=1, 2, \dots, N$ ;  $k_z=1, 2, \dots, N$ . We note that in absolute units the resonance frequency  $\omega$  is given by

$$\omega = \omega_{\text{pl}} \frac{\lambda_k}{b} \frac{\pi k_x}{\sqrt{(\lambda_k / \lambda_m)^2 + 2[1 - \cos(\pi k_z / (N+1))]}}, \quad (6)$$

where  $\omega_{\text{pl}} = [(2\pi j_c t) / (\phi_0 \epsilon \epsilon_0)]^{1/2}$  is the Josephson plasma frequency. Inserting the expressions for  $\omega_{\text{pl}}$ ,  $\lambda_k$ , and  $\lambda_m$  we find that  $\omega$  depends only on the dielectric constant  $\epsilon$ , the junction length  $b$ , and the ratios  $\lambda/t$ ,  $\lambda/d$ . An approximation of the amplitude  $\bar{e}_1$  can be found in the same way described in Ref. 10 for the single junction case. After some algebra one finds

$$\bar{e}_1 \approx J_0^2 \left[ \frac{\bar{e}_1}{2e_0} \right] F(h_{\text{ext}}), \quad (7)$$

$$F(h_{\text{ext}}) = \frac{2}{\pi} \frac{h_{\text{ext}} |\sin[\pi(h_{\text{ext}} - k_x/2)]|}{|h_{\text{ext}}^2 - k_x^2/4|}.$$

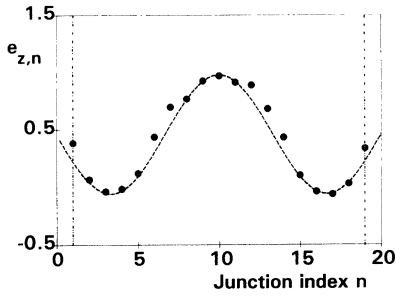


FIG. 4. Comparison of the  $z$  component of the electrical field  $e_{z,n}(x=0)$  with the sinusoidal form predicted by Eq. (5a). The dashed line is given by  $e_0 - e_1 \sin[\pi n k_z / (N+1)]$  with  $e_0 = 0.591$ ,  $e_1 = 0.52$ ,  $k_z = 3$ , and  $N = 19$ .

The maximum supercurrent (i.e., the step height) is approximately given by

$$J_{\text{DC}} \approx J_0 \left[ \frac{\bar{e}_1}{2e_0} \right]^2 J_1 \left[ \frac{\bar{e}_1}{2e_0} \right] F(h_{\text{ext}}), \quad (8)$$

where  $J_0, J_1$  are Bessel functions. The amplitudes  $e_{z,n}$  form a standing wave along  $z$  with nodes located in two imaginary junctions, which may be labeled “0” and “ $N+1$ ”. Figure 4 compares a plot of the amplitudes  $e_{z,n}$  vs  $n$  for the simulation of Fig. 2 with the sinusoidal form predicted by Eq. (5a). For this mode the values of  $e_0$  and  $\bar{e}_1$  are  $e_0 = 0.457$  and  $\bar{e}_1 = 0.52$ . From Eq. (5b) we find  $e_0 = 0.46$  and from Eq. (7)  $\bar{e}_1 = 0.55$  in very good agreement. For the maximum step height, Eq. (8) yields  $J_{\text{DC}} = 0.15$ . The step height found in the simulation is 0.1, i.e., somewhat smaller than the prediction of Eq. (8). In Table I resonance frequencies found in numerical simulations and the predictions of Eq. (5b) are compared for various resonance modes. The agreement is excellent. For large values of  $k_z$  the resonance frequency is always smaller than for small values of  $k_z$ . For small values of  $k_z$  the resonances occur approximately at

$$e_0 \approx (2\beta_c)^{-1/2} (N+1) (\lambda_k / b) (k_x / k_z)$$

in the case of strong coupling,  $\lambda_k \ll \lambda_m$ . In the case of weak coupling ( $\lambda_k \approx \lambda_m$ ) and small values of  $k_z$  the resonances occur at  $e_0 \approx \pi k_x \beta_c^{-1/2} \lambda_m / b$ , i.e., they are almost independent of  $k_z$ .

In summary, we have found that in stacked Josephson

TABLE I. Comparison of resonance frequencies obtained from numerical simulations and from the analytical formula, Eq. (5b), for resonances with various mode indices  $k_x$  and  $k_z$ ;  $s$  is the intrinsic Josephson junctions (strongly coupled  $d \ll \lambda$ ), and  $w$  is the semiconductor-insulator-superconductor multilayers (weakly coupled,  $d \approx \lambda$ ); the model parameters are given in the text.

$k_z$	$k_x$	$h_{\text{ext}}$	$e_0$ (simulation)	$e_0$ [Eq. 5(b)]	Coupling
1	5	2.5	0.75	0.75	$s$
1	4	2.5	0.6	0.61	$s$
2	10	5	0.76	0.77	$s$
2	9	5	0.68	0.69	$s$
3	9	5	0.46	0.46	$s$
3	19	10	0.98	0.98	$s$
4	19	10	0.73	0.74	$s$
1	10	5	1.07	1.09	$w$
3	10	5	1.04	1.05	$w$
6	10	5	0.78	0.78	$w$
19	10	5	0.52	0.52	$w$

junctions the interplay between Josephson vortices and collective cavity resonances leads to the formation of domains of vertically aligned vortices moving along different junctions. In particular, the situation with almost all vortices aligned was found to be stable even in the presence of a 5% parameter spread. We have obtained similar results both for parameters that are typical for artificially grown all-Nb multilayers and for parameters that are typical for intrinsic Josephson junctions in the high- $T_c$  superconductors. Different resonances can be selected by choosing appropriate external magnetic fields. For the resonance frequencies and amplitudes analytical expressions have been found. In contrast to the well-investigated two-junction case, coherent vortex motion in zero magnetic field has been found to be unstable for all investigated junction parameters. On the basis of this resonant vortex motion, flux-flow oscillators based on all-Nb junctions, as well as on intrinsic Josephson junctions, should be feasible.

The author wishes to thank A. V. Ustinov, F. Steinmeyer, and P. Müller for helpful suggestions. Financial support by the Bayerische Forschungsstiftung via the FORSUPRA consortium, and by the Bundesministerium für Forschung und Technologie via the Josephson array consortium is gratefully acknowledged.

\*Present address: Department of Physics, University of California, Berkeley, CA 94720.

<sup>1</sup>N. G. Groenbech-Jensen, D. Cai, and M. R. Samuelsen, Phys. Rev. B **48**, 16 160 (1993).

<sup>2</sup>A. V. Ustinov, H. Kohlstedt, M. Cirillo, N. F. Pedersen, G. Hallmanns, and C. Heiden, Phys. Rev. B **48**, 10 614 (1993).

<sup>3</sup>A. F. Volkov, JETP Lett. **45**, 377 (1987).

<sup>4</sup>K. L. Ngai, Phys. Rev. **182**, 555 (1969).

<sup>5</sup>R. Kleiner and P. Müller, Phys. Rev. B **49**, 1327 (1994); R. Kleiner, F. Steinmeyer, G. Kunkel, and P. Müller, Phys. Rev. Lett. **68**, 2394 (1992).

<sup>6</sup>B. Bi, S. Han, and J. E. Lukens, Appl. Phys. Lett. **62**, 2745 (1993).

<sup>7</sup>R. D. Parmentier, in *The New Superconducting Electronics*, edited by H. Weinstock and W. Ralston (Kluwer Academic, Dordrecht, 1993).

<sup>8</sup>S. Sakai, P. Bodin, and N. F. Pedersen, J. Appl. Phys. **73**, 2411 (1993).

<sup>9</sup>R. Kleiner, F. Steinmeyer, P. Müller, H. Kohlstedt, N. F. Pedersen, and S. Sakai, Phys. Rev. B (to be published).

<sup>10</sup>I. O. Kulik, Sov. Tech. Phys. **12**, 111 (1967).

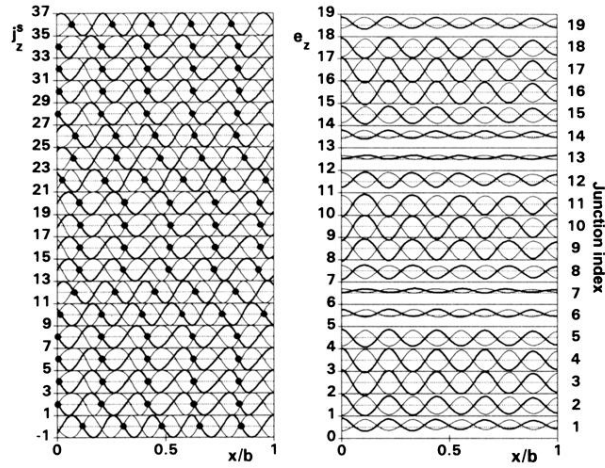


FIG. 2. Simulation of a stack of  $N=19$  strongly coupled Josephson junctions with the parameters given in the text. The left part of the figure shows the Josephson currents  $j_{z,n}^s$  vs the  $x$  coordinate of the stack. All curves have been vertically offset proportional to the junction index in order to map the junctions of the stack. Thick and thin curves correspond to two different values of the normalized time  $\tau=26$  and  $32$ . In order to show that the Josephson vortices move in three aligned domains the centers of mass of the vortices have been marked with black dots for  $\tau=26$ . The right part of the figure shows the electrical field component in  $z$  direction  $e_{z,n}$ . The figure shows that a two-dimensional standing wave pattern has developed. In the  $n$ th junction the electrical field is approximately of the form  $e_n \approx e_0 + \bar{e}_1 \sin[\pi k_z / (N + 1)] \cos(\pi k_x x) \cos(e_0 \tau)$  with  $k_x=9$  and  $k_z=3$ .